



CaCO₃-coated indoxacarb deep eutectic solvent complexed with diatomaceous earth improves insecticidal activity against the red imported fire ants

Jiantao Fu ^{a,b}, Junfang Wang ^a, Zewen Ma ^a, Di Yuan ^a, Yunfei Zhang ^a, Lanying Wang ^a, Yanping Luo ^{a,*}

^a School of Tropical Agriculture and Forestry, Hainan University, Danzhou, Hainan 570228, China

^b Institute of Nanfan & Seed Industry, Guangdong Academy of Sciences, Guangzhou, Guangdong 510316, China



ARTICLE INFO

Edited by Anita Jemec Kokalj

Keywords:

Red imported fire ants
Deep eutectic solvent
Indoxacarb
CaCO₃-loaded nanoparticles
Diatomaceous earth

ABSTRACT

The red imported fire ants (RIFAs) are a globally important invasive pest that severely affects the ecosystem and human health, and its current control is primarily through chemical pesticides. However, the extensive use of chemical pesticides causes environmental problems, and alternative strategies for controlling this pest are being explored. In our study, we aimed to design a deep eutectic solvent (DES)-CaCO₃ system in which RIFAs were used as target insects to increase the lethal activity and behavioural regulation effects on RIFAs via contact and feeding. Indoxacarb (IDC) was made into DESs with three fatty acids, oleic acid (OA), linoleic acid (LA), and linolenic acid (LNA), which showed a significant increase in lethal activity against worker ants compared with IDC. OA@IDC@CaCO₃, LA@IDC@CaCO₃, and LNA@IDC@CaCO₃ nanoparticles were prepared via interfacial precipitation. Characterization of the structures of the three pesticide-carrying nanoparticles revealed that all three fatty acid eutectic solvents formed spherical CaCO₃ nanoparticles, with average particle sizes between 0.59 and 0.90 μm, which increased with increasing degree of fatty acid unsaturation. The pesticide loading ranged from 2.13 % ~ 3.43 %, and the surfaces were all positively charged and well dispersed. OA@IDC@CaCO₃ was relatively more effective and was able to dramatically inhibit the abandonment and foraging behaviours of RIFAs, prolong the time required for these behaviours, and decrease the number of feeding worker ants and the amount of food consumed. OA@IDC@CaCO₃ was subsequently compounded with diatomaceous earth (DA), and spiked into baits, which significantly increased the contact and feeding activity of worker ants, inhibited the feeding, digging, and corpse-discarding behaviours of RIFAs. In the field trial, the combined control effect of the DA + OA@IDC@CaCO₃ group was 83.38 %, which was greater than the 69.65 % of the commercial agent control group. In this study, IDC bait was co-prepared by using acid as a comelting solvent, CaCO₃ as a coating, and DA as a pesticide adjuvant, which improved the activity against RIFAs, prolonged the holding period of IDC, and improved the prevention and control of RIFAs. Therefore, our research provides a simple and feasible approach for designing and constructing novel nanopesticides for RIFAs control.

1. Introduction

RIFAs, *Solenopsis invicta* Buren, are one of the most dangerous invasive species in the world and has invaded many countries, including Australia, China, Japan, and Italy (Menchetti et al., 2023), causing significant damage to human health, the ecological environment, and agricultural and forestry production (Lei et al., 2019). In the United States, the annual loss from damage repair, medical treatment, and

control of RIFAs exceeds US\$6 billion (Bertelsmeier et al., 2017), and the loss in China exceeds \$25 billion (Xu et al., 2022). The safe and effective management of RIFAs has emerged as a critical global challenge. Chemical pesticides, particularly baits and contact insecticides containing flumioxazin, abamectin, and indoxacarb, remain the primary means of RIFAs prevention and control (Yang et al., 2023).

IDC, a broad-spectrum new type of oxadiazine insecticide with the advantages of insolubility in water, low toxicity, excellent control

* Correspondence to: School of Tropical Agriculture and Forestry, Hainan University, Danzhou, Hainan, China.

E-mail address: yanpluo2012@hainanu.edu.cn (Y. Luo).

effects, fast effects, and low usage, is the most widely used pesticide in China to control RIFAs (Wang et al., 2020a). It works primarily by blocking sodium channels in target pest nerve cells via N-demethoxy carbonyl metabolites, resulting in midgut disintegration (Jaleel et al., 2021). It is used not only to control lepidopteran pests but also to control a variety of other insects, such as ants, cockroaches, leafhoppers, and aphids (Wing et al., 2000). However, conventional pesticide formulations are lost directly to the environment during use because of drift or degradation by light, microorganisms, and temperature, with only 10–15 % of the pesticide reaching the target site and an actual utilization rate for biological target uptake of less than 0.1 % (Fukamachi et al., 2019). Blind application can also cause severe environmental issues, such as the death of nontarget organisms such as bees, ladybirds, and fish, as well as air, water, and soil pollution, which can endanger human health (Gruber et al., 2022). IDC bait has similar issues during application, such as poor stability, easy ultraviolet degradation, a short persistence period, high toxicity to aquatic organisms, and other shortcomings, and long-term use for red fire ants results in resistance. As a result, the development of new pesticides is a key area of technological development for RIFAs control (Zheng et al., 2022). The development of new active chemicals is expensive and difficult to achieve in a short period of time; thus, improving highly active pesticide formulations is a cost-effective way to delay or overcome resistance (Bilal et al., 2020).

Some nanomaterials have been shown to have insecticidal activity; for example, raw and calcined diatomaceous earth have been used as natural insecticides to eliminate common grain storage pests and increase lethality against sawtooth grain beetles, *Tribolium ferrugineum* (Li et al., 2022). Furthermore, nanomaterials and pesticides have synergistic effects, and multiwalled carbon nanotubes (MCN) were found to enhance the effects of dibutyl phthalate on the early life stages of zebrafish (Chen et al., 2023). Coexposure of oxidized MCN with furadan was found to affect shrimp metabolism and increase pesticide toxicity, possibly due to the ability of carbon nanotubes to adsorb and transport pesticides in organisms, resulting in a synergistic effect (Alves et al., 2022). DA and MCN can increase the effectiveness against RIFAs and inhibit their colony behaviour (Ma et al., 2024).

Nanopesticide delivery systems have also shown great potential for RIFAs control. Feeding with biodegradable chitosan (CS) and carboxymethyl chitosan (CMCS) organic polymer nanoparticles resulted in the inhibition of feeding, growth, and development of RIFAs; significant dilation of the midgut; and a reduction in midgut digestive enzyme activities (Zheng et al., 2021). The pH-sensitive rotenone nanoparticles prepared with chitosan and carboxymethyl chitosan exhibited photo-protective and slow-release effects on rotenone, which significantly enhanced the insecticidal activity of rotenone against RIFAs (Zheng et al., 2022). In addition, by complexing β -cyclodextrin with zeolite imidazole skeleton-90 (ZIF-90) nanoparticles loaded with indoxacarb to construct a pesticide release system with a dual stimulation response of pH and α -amylase, the pesticide release system rapidly releases indoxacarb under acidic and amylase-catalysed conditions, reduces the photodegradation of indoxacarb, prevents the premature release of the active ingredient, and interferes with the response to RIFAs by increasing the feeding and damaging the intestinal cell metabolism of RIFAs by increasing the degree of feeding and damaging intestinal cells, thus increasing the toxicity of indoxacarb to RIFAs (Yang et al., 2023). Although NiCoNC has no insecticidal activity against RIFAs, it increases the insecticidal activity of fludioxonil by increasing their sensitivity to insecticides through entry into the gut (He et al., 2023a).

In addition, traditional organic solvents have the disadvantages of being highly volatile, toxic, and environmentally unfriendly, and replacing traditional solvents with green solvents has become an irreversible research trend. In this context, DES has attracted public consciousness, and as a new type of green solvent, they have received much attention (Cao and Su, 2021). DESs are emerging green reactive solvents that are liquid at room temperature and are low-eutectic mixtures composed of hydrogen-bonding donors and hydrogen-bonding

acceptors combined in a specific molar ratio. The melting point of the mixture is lower than that of the individual components (Omar and Sadeghi, 2023). DES, which are safe, naturally nontoxic, nonflammable, nonvolatile, thermally stable, sustainable, biodegradable, and low-cost, almost meet the criteria of green solvents and are widely used in extraction, pharmaceuticals, fuel desulfurization, metallurgy, electro-deposition, biocatalysis (Abro et al., 2022), and nanomaterials because of their numerous advantages, including low cost, ease of preparation, environmental friendliness, biocompatibility, and structural designability, allowing them to outperform similar solvents and organic solvents (El Achkar et al., 2021). Furthermore, with the development of nanotechnology, nanoencapsulation using DES has become increasingly feasible. Mou et al. reported a new method for producing graphene-encapsulated Ni₂P by designing a DES and performing a simple annealing treatment (Mou et al., 2019). β -Carotene was encapsulated in whey protein concentrate capsules via an emulsion electrospray technique using DES as a solvent. DES has high solubilization, extraction, and stabilization capabilities for a wide range of compounds, especially poorly water-soluble compounds, with great potential for encapsulating and stabilizing highly insoluble bioactive compounds (Basar et al., 2020). Curcumin was encapsulated in pH-responsive alginate-chitosan hydrogel beads via DES for intestinal-targeted delivery (Silva et al., 2021). Li et al. used DES as a reaction solvent in conjunction with water to rapidly encapsulate cytochrome c (Cyt c) in a COF covalent organic framework under ambient conditions, and this encapsulation strategy demonstrated excellent resistance to organic solvents and recovery stability (Li et al., 2023a). Li et al. demonstrated the ability of DES to increase the permeability of rigid nanoparticles (Li et al., 2023b). Shah et al. reported several synthetic and natural DESs that increased the solubility of the insoluble drug DTX, which was reduced in crystallinity and stably encapsulated in DES through hydrogen bonding, and was later developed as a self-emulsifying formulation that formed nanoscale spheres upon dilution (Shah et al., 2024).

The literature on the insecticidal activity of DESs is relatively sparse, particularly regarding their preparation using chemical pesticides. This study aims to develop a novel DES–CaCO₃ system to increase both the lethal activity and behavioural regulation effects on RIFAs through contact and feeding methods. Notably, our DES–CaCO₃ system, when combined with the application of insecticidal compounds (IDCs) and deltamethrin (DA), significantly improved the efficacy. Therefore, this research offers a straightforward and viable strategy for the effective control of RIFAs, providing new research perspectives and technical frameworks for the design and development of nanopesticides targeted at RIFAs management.

2. Materials and methods

2.1. Reagents and materials

Yulin Chengtaiheng Biotechnology Co., Ltd., in China provided 96 % of the technical IDC (TC) purchased. DA was purchased from Yirui Stone Group in France. Sinopharm Chemical Reagent Co., Ltd., in China supplied CaCl₂·2 H₂O and Na₂CO₃. MCN was purchased from Jiangsu Xianfeng Nanomaterials Technology Co., Ltd., in China. OA, LN, LNA, fatty methyl esterSulfonates (FMES), and polytetrafluoroethylene (PTFE) were purchased from Shanghai Macklin Biochemical Technology Co., Ltd., in China.

2.2. Insects

RIFAs were collected from the new agricultural research base of Hainan University located in Danzhou city, Hainan Province, China. The entire nest was excavated and transported to the laboratory in a 20-litre plastic bucket, the inner walls of which were coated with polytetrafluoroethylene (PTFE) micropowder to prevent the escape of the ants (Ning et al., 2019). After rearing in the laboratory for 1–2 days, tap

water was gradually added to the bucket until all the soil was submerged (Collignon et al., 2023). As the RIFAs colony floated to the surface, the ants were carefully collected via a fishing net and transferred to a plastic box (40 cm × 30 cm × 15 cm), whose inner walls were coated with PTFE micropowder. The box contained a 10 % sucrose solution and ham sausage, which served as water and food sources. The ants were maintained indoors at a temperature ranging from 24 to 28 °C and a humidity ranging from 60 % to 80 %. Worker ants of uniform size (body length was 3.0–4.0 mm, head width was 0.7–0.9 mm) were chosen for the activity test experiment.

2.3. Preparation of DESs

After fully mixing IDC and acid at a molar ratio of 1:1, the mixture was placed in a vacuum drying oven, heated under vacuum conditions at 80 °C for 2 h, and then heated at 100 °C for 2 h to obtain OA@IDC, LA@IDC, and LNA@IDC.

Preliminary screening of the acid was performed by adjusting the proportion of the eutectic solvent prepared with IDC, screening IDC: acid ratios of 1:2, 1:3, and 1:5, as well as the eutectic solvent performance with a 1:1 mixture of acid, and screening the eutectic solvent with better stability and dispersibility for coating.

OA@IDC, LA@IDC, and LNA@IDC are insoluble in water; therefore, some green emulsifiers were tested to improve the dispersion of eutectic solvents in water for later coating. After 100 µL of DES was mixed with 1 mL of emulsifier in 40 mL of distilled water, the dispersion and stability were measured after 1 h.

2.4. Preparation of the DES–CaCO₃ system

A total of 100 µL of eutectic solvent was combined with 1 mL of FMES, mixed thoroughly, and dissolved in 50 mL of 0.04 mol/L calcium chloride solution (containing 10 % ethylene glycol). Fifty millilitres of 0.04 mol/L Na₂CO₃ solution (containing 10 % ethylene glycol) was added dropwise at 1000 rpm with stirring, the mixture was stirred for 1 h, and then the mixture was incubated for 12 h. After 12 min of agitation, the mixture was rotated at 10,000 rpm for 12 min. The samples were subsequently washed three times and dried overnight at 70 °C in a vacuum drying oven.

2.5. Characterization of the DES–CaCO₃ system

2.5.1. Pesticide loading capacity

10 mg of loaded nanoparticles were weighed and added to 10 mL of anhydrous ethanol, dispersed with ethanol, sonicated for 30 min to release IDC, and the absorbance was measured with a UV spectrophotometer to determine the loaded amount. All samples have been filtered with a 0.22 µm nylon syringe filter before being examined by a high-performance liquid chromatography (HPLC) system (Shimadzu, Japan) with a UV detector. Prepare 1 mg/mL IDC-acetonitrile solution as masterbatch, dilute the solution to 0.5 µg/mL, 1 µg/mL, 2 µg/mL, 5 µg/mL, 10 µg/mL, 20 µg/mL by gradient dilution, repeat three times, and then use the HPLC to measure peak area. The detection conditions are as follows: The C18 column (250 × 4.6 mm, 5 µm, Agilent, USA) was eluted with a mobile phase composed of aqueous solution (containing 0.1 % phosphoric acid, v/v) and acetonitrile (containing 0.1 % phosphoric acid, v/v) (75:25, v/v) at a flow rate of 1.0 mL/min. The injection volume was 10 µL and the column temperature was 30 °C. The chromatogram was observed at 280 nm. The HPLC standard curve were presented in Fig. S1 in the Supporting Information. Pesticide loading capacity and Pesticide loading efficiency (DLE) were calculated according to the following formula:

$$\text{PLC (\%)} = [\text{weight of pesticide loaded} / (\text{weight of polymer} + \text{pesticide used})] \times 100\%$$

$$\text{PLE (\%)} = (\text{weight of loaded pesticide} / \text{weight of input pesticide}) \times 100\%$$

2.6. Scanning electron microscopy (SEM)

10 mg of pesticide-loaded nanoparticles were weighed, 10 mL of anhydrous ethanol was added, and the mixture was ultrasonicated for 10 min. Then, 10 µL droplets of the dispersion on the surface of monocrystalline silicon wafers were aspirated, naturally air-dried, sprayed with gold, and observed via a field emission scanning electron microscope S-4800. The diameter of the nanoparticles in the SEM images was measured via ImageJ (V 1.8.0), the diameters of 200 nanoparticles were randomly selected and measured, histograms of the frequency distributions of the particle sizes were plotted, and the average particle size was determined.

2.6.1. Particle size distribution and potential determination

10 mg of pesticide-loaded nanoparticles were weighed, 10 mL of anhydrous ethanol was added, and the mixture was ultrasonically dispersed for 10 min. The hydrated particle size, polydispersity index (PDI), and surface zeta potential of the materials in aqueous solution were determined via nanoparticle size and a zeta potential metre, and the measurements were repeated three times for each treatment.

2.6.2. Determination of the cumulative release rate

0.2 mol/L pH=7 PBS buffer (sodium dihydrogen phosphate and disodium hydrogen phosphate) was used. At an acetonitrile: buffer ratio of 3:7, 95 mL was removed and placed in a glass bottle as the dissolution medium. One milligram of IDC and 1 mg of OA@IDC@CaCO₃ with IDC as the active ingredient were weighed into a dialysis bag, and 5 mL of dissolution medium was added to the bag, which was stirred at 100 rpm. After stirring for 0.5, 1, 2, 4, 6, 8, 10, 12, 16, 24, 36, and 48 h, 1 mL of solution was drawn from a glass vial, passed through a 0.22 µm organic filter membrane, and then the IDC content was detected via HPLC system to calculate the dissolution rate. The detection method is the same as mentioned above. Following each sample, 1 mL of dissolution medium was added to the glass vial, ensuring that the total volume remained consistent.

2.7. Bioactivity test

2.7.1. Contact activity

300 worker ants were allowed to crawl in a 100 mL beaker for 2 h after 1 g of bait was placed in its bottom and evenly distributed. After 2 h, 150 workers were randomly assigned to three plastic boxes (168 × 115 × 70 mm (length × width × height)) and fed a 10 % sucrose aqueous solution. The number of worker deaths was recorded at 24-h intervals, and each treatment was replicated three times. The bait consisted of 10 % sucrose, 5 % chicken meal, 5 % fish meal, and 10 % peanut oil; the active ingredients were added in the appropriate ratios and the remainder was corn meal. (16 × 12 × 9.5 cm)

2.7.2. Feeding activity

50 worker ants of the same size were randomly selected and placed in the plastic box mentioned above coated with PTFE powder and starved for 6 h. A total of 0.5 g of prepared bait was weighed and placed in the lid of a 3 cm Petri dish, which was then placed in a plastic box for RIFAs to feed on, as well as water for feeding. The number of worker deaths was recorded every 24 h. Each treatment was administered three times.

2.7.3. Horizontal transfer effects of active ingredients

To determine the potential transfer effect of the active ingredient from dead to untreated live ants and referring to Dantas et al. (2023), an experiment was designed using a ratio of dead: live ants = 1:5. Worker ants were exposed to the compound bait for 24 h, and dead individuals were chosen for subsequent experiments. A blank control group of dead ants was obtained by freezing at -20 °C for 30 min in a refrigerator.

50 worker ants without any treatment and 10 treated dead ants were added to a round plastic box (9 cm diameter) coated with PTFE powder

and fed a 10 % sucrose aqueous solution. The number of dead ants in each box was counted at 12 h intervals. Each treatment was repeated five times.

2.8. Behavioural tests

2.8.1. Digging behaviour

In accordance with He et al. (2023b), the river sand was screened with a 40-mesh sieve, washed with water, dried again after 12 h, and weighed twice, and an error of 0.02 g was considered acceptable. Four 2 mL glass bottles were glued under 15 cm plastic petri dishes as supports. The distance between the glass vials and the centre of the Petri dish was 5 cm, and a 3 mm diameter hole was drilled in the centre of the two vials at opposite corners. Two glass vials with drilled holes were filled with sand, and the other two vials without drilled holes were used as supports. The inner walls of the Petri dishes were coated with PTFE to prevent the ants from escaping. The sand used for filling was mixed with water at a certain ratio (7.68 mL of water + 120 g of sand) to fill the drilled vials (containing 3.19 g of wet sand, which is approximately 3 g of dry sand). Three hundred worker ants and 30 juveniles were selected to be placed in a plastic box with 1 g of bait for feeding. From the worker ants that were fed for 24 h, 50 worker ants were randomly selected to be placed into Petri dishes and fed with water, and each treatment was repeated three times. After 24 h, the remaining sand in the vials was collected and dried in a vacuum drying oven to a constant weight, and the mass of the excavated sand was calculated.

2.8.2. Necrophobic behaviour

The worker ants moved the dead individuals out of the nest and piled them in a corner, a behaviour called necrophagy. In accordance with Ning et al. (2020), 500 worker ants, 50 juvenile ants, and 5 reproductive ants were kept in a plastic box with an artificial nest before the test. After 24 h of starvation treatment, 1 g of bait was weighed and placed in a 3 cm Petri dish, which was placed 5 cm from the artificial nests, and each nest was fed highly active nanomaterials for 24 h, with the addition of water. Twenty-four hours later, 40 dead worker ants were placed 5 cm from the nests. The time taken for the worker ants to find the carcasses, the time taken to start carrying the carcasses and the time taken for all the carcasses to be removed from the perimeter of the artificial nest were recorded.

2.8.3. Foraging behaviour

In reference to Huang et al. (2018), the foraging ability of a colony after RIFAs were fed baits was assessed. An artificial ant nest was established, and after 24 h of starvation, highly active nanomaterials were used for feeding for 24 h. Twenty-four hours later, the bait was removed, 1 g of ham sausage was added, and the ham sausage was replaced every 24 h to maintain the attractiveness of the food. The replaced ham hocks were weighed to calculate the weight of the ham hocks taken and placed in a plastic box free of ants to eliminate the effect of natural air drying. Fresh water was added to the feed. The time when the first worker ant found the ham sausage and the time when the worker ant started to carry it were recorded. The weight carried by the worker ants was recorded at 24-h intervals. The number of worker ants on the ham hock was recorded at 10-minute intervals within 60 min of the first addition of the ham hock.

2.9. Field experiment

The field experiment was conducted at Danzhou Experimental Base of Hainan University ($E 109^{\circ}30'32.872''$, $N 19^{\circ}30'20.574''$), an area of high RIFAs occurrence was selected for the field test, with an area of approximately 300 m^2 containing at least five live ant nests within the test area. The test baits were prepared according to previous formulations. Four treatment groups were established: the commercial formulation treatment group (0.05 % IDC), the DA and CaCO_3 treatment

group, the OA@IDC@ CaCO_3 + DA treatment group, and the blank treatment group. The worker ants in the nests were trapped via the baiting method 1 d before application, and the basal number was counted. Each nest was baited with 20 g of bait, and each treatment was replicated three times. On the 7th, 14th, 21st, and 28th d after the treatment, worker ants were trapped via the hammering bait method, the control effects on worker ants and live ant nests were calculated, and the ant nests were excavated after the 28th day of baiting to calculate the control effect on the ant colony and the comprehensive control effect. The calculation method used GBT 17980.149–2009 Pesticide Field Efficacy Test Guideline (II) Part 149: Insecticide Control of Red Fire Ants (Standardization Administration of the People's Republic of China, 2009).

2.10. Statistical analyses

All data, including contact, feeding activity, and effects on behaviour, are presented as the means \pm standard deviation (SD) of three replicates. The results were analysed via one-way analysis of variance (ANOVA). Tukey's HSD test was used to separate means at $p \leq 0.05$. Analyses were performed via SPSS 26.0, and graphs were generated via Origin 2022.

3. Results

3.1. Preparation of the DESs

We conducted a literature review and selected 30 kinds of fatty acids to prepare DES with IDC at a molar ratio of 1: 1 (Table S1). The eutectic solvents prepared from oleic acid, linoleic acid, linolenic acid, octanoic acid, lauric acid, myristic acid, hexadecanoic acid, behenic acid, stearic acid, and 12-hydroxystearic acids with IDC TC were in the liquid state when heated at 100°C , and there was partial deposition of solid, which may have been IDC deposition. Lactic acid, 2-chlorobenzoic acid, sorbic acid, humic acid, oxalic acid, and IDC TC were mixed in the solid-state and did not melt when heated at 100°C . The other acids were not able to produce eutectic solvents, as they were still clearly layered under heating at 100°C . The molar ratios of acid to IDC TC were subsequently adjusted to 2:1 and 3:1, and only the DESs of oleic acid, linoleic acid, linolenic acid, and octanoic acid were liquid at room temperature (Table S2). The molar ratio of acid to indoxacarb was gradually increased to 5:1, and its stability was measured after 24 h in water. Table S3 shows that the eutectic solvent of linoleic acid, linolenic acid, and indoxacarb was relatively stable. As a result, the DES was prepared using these three acids and indoxacarb.

Owing to the greater structural similarity of oleic acid, linoleic acid, and linolenic acid, these three acids were used for the subsequent preparation and coating of DES. One hundred microlitres of each of the three eutectic solvents was dissolved in 1 mL of methanol, added to 50 mL of distilled water, dispersed homogeneously, and left to remain for 12 h without solid precipitation. The pictures before and after the preparation of the OA@IDC, LA@IDC, and LNA@IDC DESs are shown in Fig. S2 A, B, and C. The IDC contents of the OA@IDC, LA@IDC, and LNA@IDC DESs were determined to be 29.4 %, 36.8 %, and 25.7 %, respectively (Fig. S2 D). OA@IDC, LA@IDC and LNA@IDC were dispersed in water by adding 1 % cosolvent methanol to obtain a solution of IDC at 25 $\mu\text{g/mL}$, which was used to determine the feeding toxicity to worker ants. The results revealed that the mortality of worker ants in the OA@IDC, LA@IDC, and LNA@IDC DES groups was significantly greater than that in the blank control, methanol control, and IDC TC-treated groups (Fig. S2 E).

3.2. Characterization of DES@ CaCO_3

The morphologies of the OA@IDC@ CaCO_3 , LA@IDC@ CaCO_3 , and LNA@IDC@ CaCO_3 nanoparticles were observed via SEM, and the

particles were round, uniform in size and had a rough surface (Fig. 1A, B, C, D, E, F). CaCO_3 was deposited on the surface of the eutectic solvent droplets, forming a single-shell microcapsule. Furthermore, the particle size distributions of $\text{OA}@\text{IDC}@\text{CaCO}_3$, $\text{LA}@\text{IDC}@\text{CaCO}_3$, and $\text{LNA}@\text{IDC}@\text{CaCO}_3$ were analysed via dynamic light scattering analysis and were 0.4–0.9, 0.6–1.4, and 0.4–1.1 μm , respectively (Fig. 1G, H, I), and the average particle sizes of $\text{OA}@\text{IDC}@\text{CaCO}_3$, $\text{LA}@\text{IDC}@\text{CaCO}_3$, and $\text{LNA}@\text{IDC}@\text{CaCO}_3$ were $0.59 \pm 0.10 \mu\text{m}$, $0.73 \pm 0.12 \mu\text{m}$, and $0.90 \pm 0.15 \mu\text{m}$, respectively. Moreover, as shown in Fig. 1J, the pesticide loading efficiency of IDC in the final $\text{OA}@\text{IDC}@\text{CaCO}_3$, $\text{LA}@\text{IDC}@\text{CaCO}_3$, and $\text{LNA}@\text{IDC}@\text{CaCO}_3$ nanoparticles was calculated

to be $3.22 \pm 0.16 \%$, $3.43 \pm 0.14 \%$ and $2.13 \pm 0.19 \%$, respectively. As shown in Fig. 1K, the zeta potential of three nanoparticles in PBS was measured to investigate the interactions among different components. The surface charge of the CaCO_3 solution was 20.76 mV. The $\text{OA}@\text{IDC}@\text{CaCO}_3$, $\text{LA}@\text{IDC}@\text{CaCO}_3$, and $\text{LNA}@\text{IDC}@\text{CaCO}_3$ nanoparticles had surface charges of 29.52, 29.87, and 40.97 mV, respectively, and the absolute value of the zeta potential increased, indicating that the CaCO_3 encapsulated the DESs. The values of the polymer dispersity index (PDI) of the three types of nanoparticles ranged from 0.09 to 0.30, which indicated that the distribution of the nanoparticles was more concentrated and that there was no adhesion or agglomeration

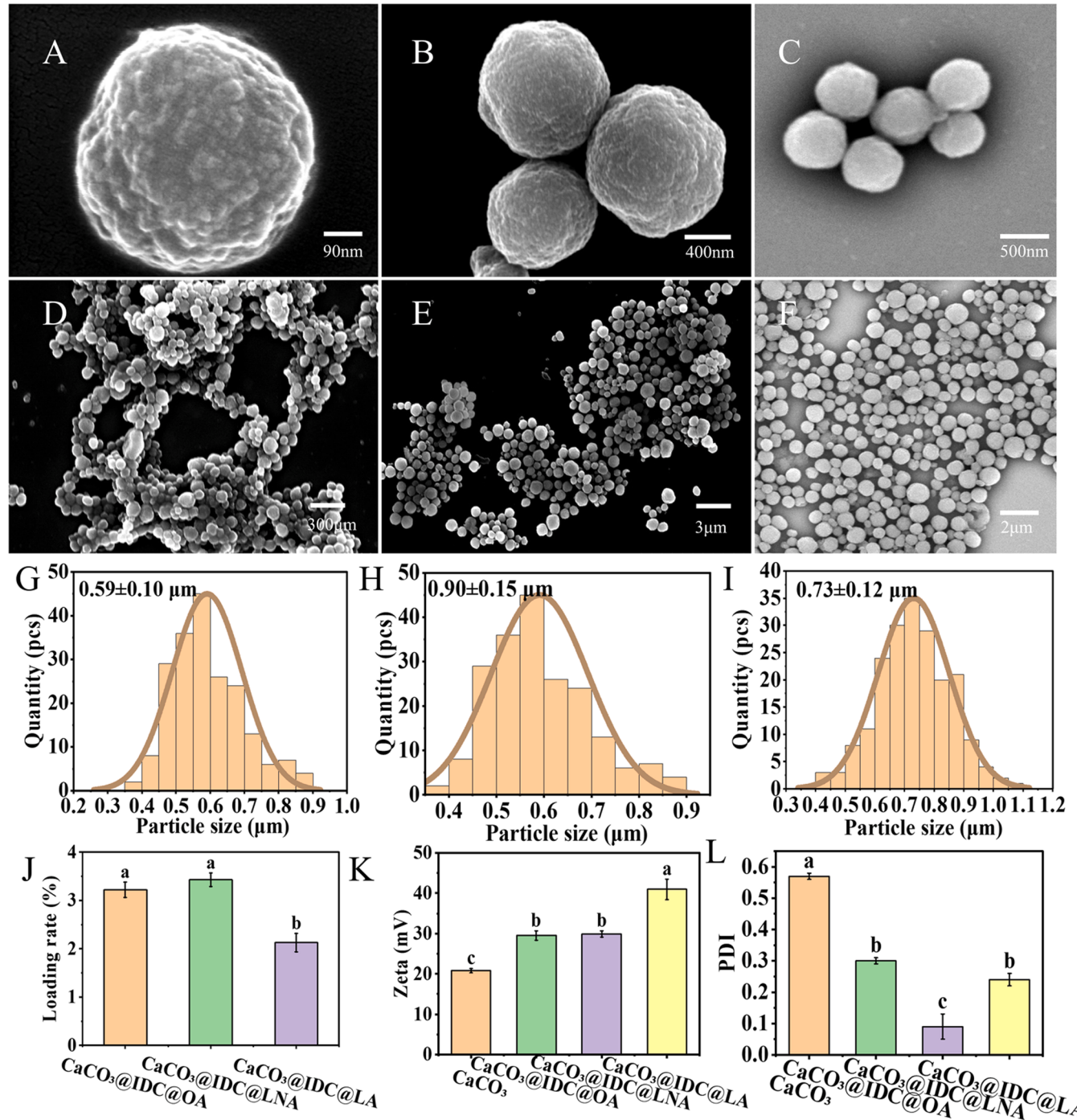


Fig. 1. SEM images, the particle size distribution of $\text{OA}@\text{IDC}@\text{CaCO}_3$ (A, D, G), $\text{LA}@\text{IDC}@\text{CaCO}_3$ (B, E, H), $\text{LNA}@\text{IDC}@\text{CaCO}_3$ (C, F, I), respectively. J: DLE of IDC. K: The zeta potential. L: PDI. Data are presented as mean \pm SE. Different letters above bars indicate significant differences at $p < 0.05$ level based on Tukey's t-test ($n = 3$).

(Fig. 1L).

3.3. Toxicity test of DES@CaCO₃

To evaluate the feeding activity of pesticide-loaded nanoparticles on worker ants, we determined the mortality rates of worker ants after 12, 24, 36, 48, 60, and 72 h of treatment at four IDC concentrations, including 0.05 %, 0.01 %, 0.005 % and 0.0025 %, and the results are shown in Fig. 2. At an IDC concentration of 0.05 %, the three types of CaCO₃ loaded nanoparticles showed almost no difference compared with the IDC TC group (Fig. 2A), RIFAs mortality ranged from 81.33 % to 88.67 % after 72 h of treatment. At an IDC content of 0.01 %, the mortality rates of the OA@IDC@CaCO₃, LA@IDC@CaCO₃, and LNA@IDC@CaCO₃ treatment groups were significantly greater than those of the IDC TC group after 24, 36, 48, 60, and 72 h (Fig. 2B), as an example, after 72 h of treatment, the mortality rate in the IDC TC group was 53.33 %, while the mortality rate in the OA@IDC@CaCO₃ and LNA@IDC@CaCO₃ treatment groups was 64.67 %and 68.00 %, which was significantly higher than that in the original treatment group. At an IDC concentration of 0.005 %, the LA@IDC@CaCO₃ treatment group did not show a significant difference in mortality rate for the same treatment time compared with the IDC TC group (Fig. 2C). However, after 36 h of treatment, The mortality rate of OA@IDC@CaCO₃ and LNA@IDC@CaCO₃ treatment groups was significantly higher than that in the IDC TC group. After 72 h, the mortality rate in the OA@IDC@-CaCO₃ treatment group was 42.00 %. At the IDC level of 0.0025 %, the mortality was higher in the OA@IDC@CaCO₃ treated group than in the IDC TC treatment group, but the difference was not significant. After 72 h of treatment, the mortality rate was less than 20 % in each

treatment group (Fig. 2D). These findings indicate that pesticide-loaded nanoparticles have excellent feeding toxicity compared with IDC TC at low concentrations.

3.4. Behavioural tests of DES@CaCO₃

To further explore the effects of pesticide-carrying granules on the behaviour of RIFAs, behaviours such as foraging, digging, and carcass abandonment were observed and recorded, as shown in Fig. 3. After 24 h of feeding, the OA@IDC@CaCO₃ and LA@IDC@CaCO₃ treated groups significantly prolonged the time required for worker ants to find food compared with the IDC TC group, but there was no significant difference between the LNA@IDC@CaCO₃ treatment group and the control group (Fig. 3A). Ants in the OA treatment group took the longest time to find food at 44.67 s. In terms of the time required to locate and begin transporting the food, all three pesticide-loaded pellet treatment groups took longer than the control group. Among them, the OA@IDC@CaCO₃ treatment group had the longest duration, taking 313 s to begin the process, compared to the IDC TC group (Fig. 3B). Compared with the blank control, all the treatment groups presented a significantly lower number of foraging worker ants within 20 min after treatment. There was no significant difference between the three pesticide-loaded nanoparticle treatment groups and the IDC TC group (Fig. 3C); for food consumption, all the treatment groups presented a decrease in food intake compared with the blank control (Fig. 3D), after 10 min, the OA@IDC@CaCO₃ took the least amounts of food, 0.037 g. As shown in Fig. 3E, after 24 h of feeding at IDC concentrations of 0.0025 % and 0.001 %, the digging weight by worker ants was significantly lower in all the treatments compared with the blank control. At an

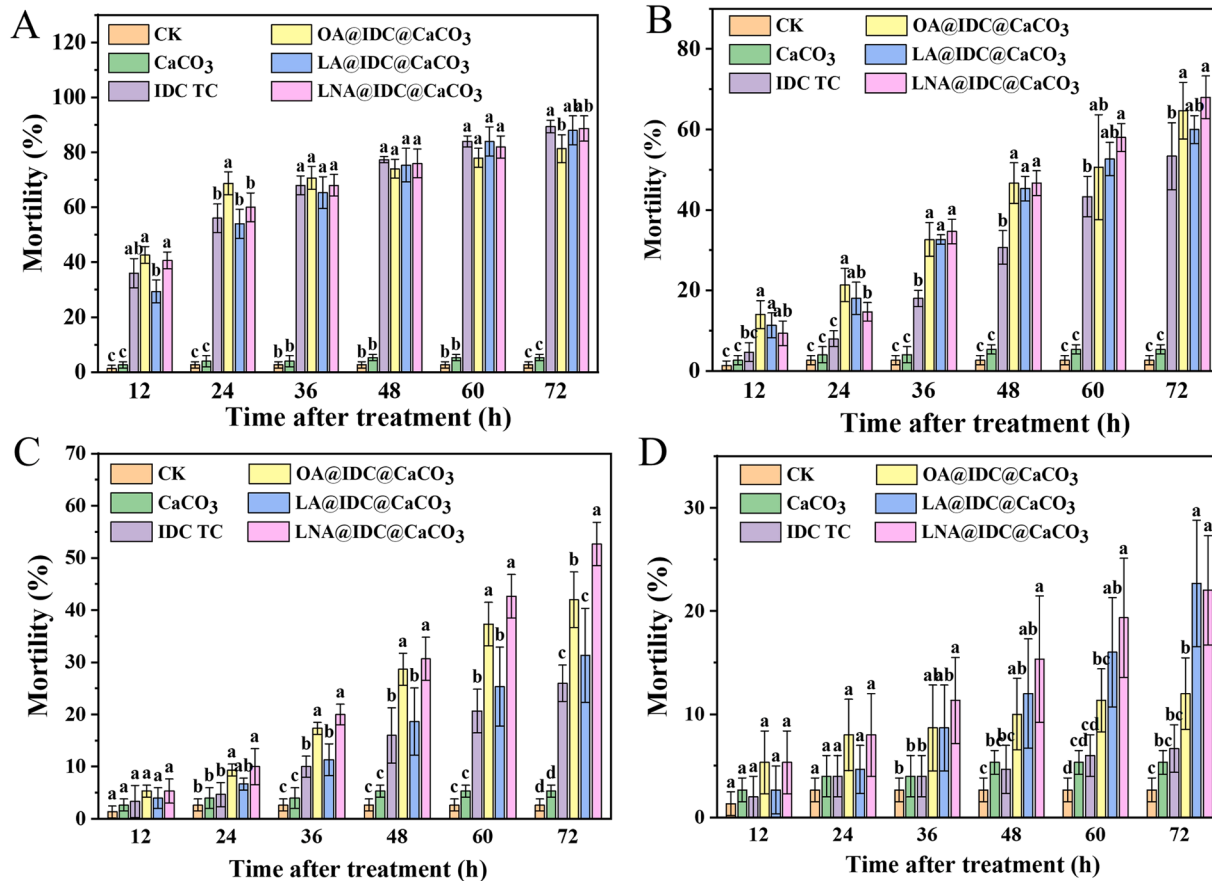


Fig. 2. Feeding activity of CaCO_3 -loaded nanoparticles with different IDC contents on worker ants. A: 0.05 %, B: 0.01 %, C: 0.005 %, D: 0.0025 %. Data are presented as mean \pm SD. Different letters above bars indicate significant differences in mortality rate at the same time among treatments due to nanomaterials effects at $p < 0.05$ level based on Tukey's *t*-test ($n = 20$).

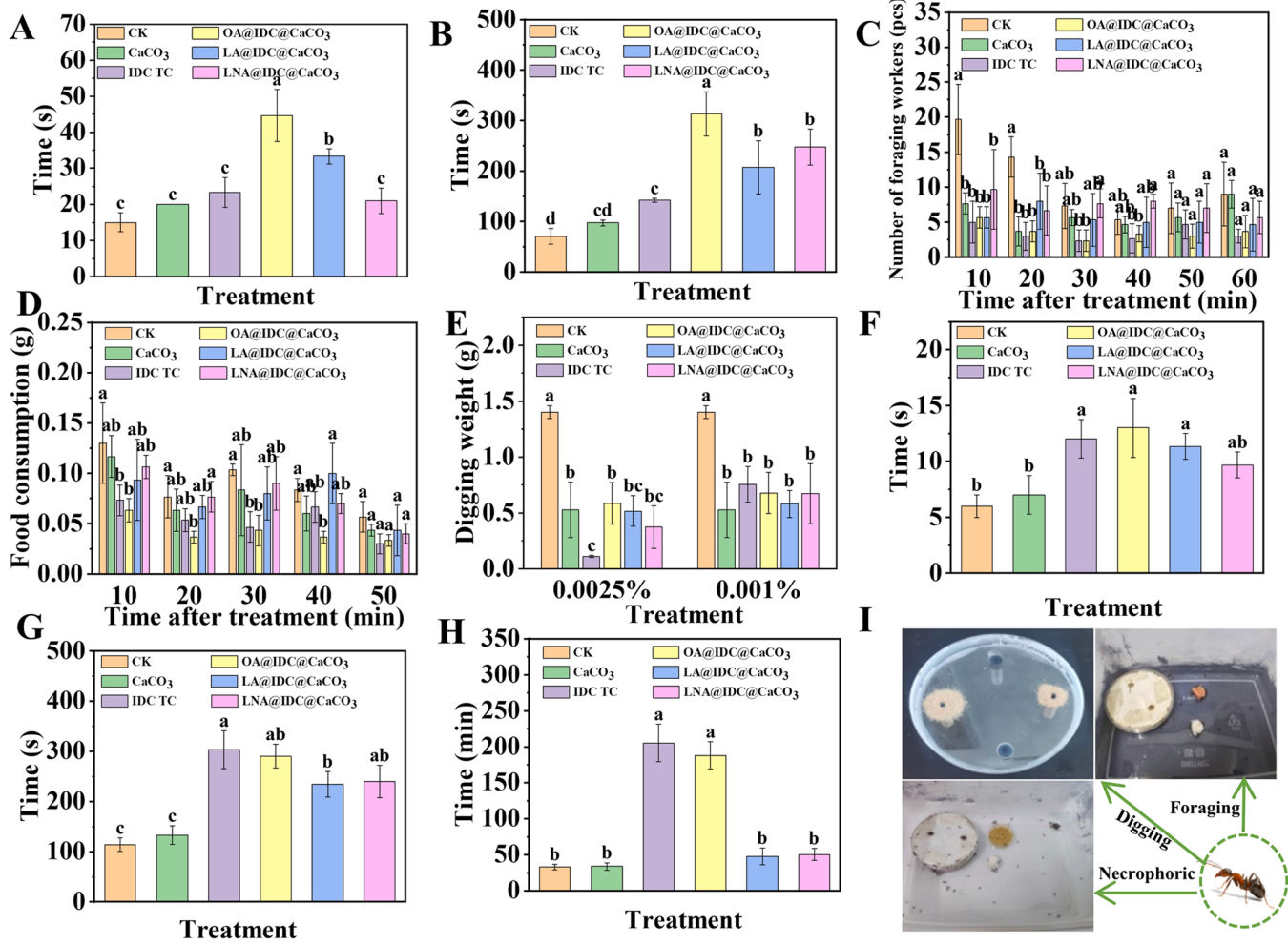


Fig. 3. Effects of pesticide-carrying nanoparticles on foraging behavior, digging, and carcass disposal of worker ants. A: time taken by worker ants to find food; B: time taken by worker ants to start carrying food; C: number of worker ants carrying food; D: weight of food carried by worker ants; E: amount of excavation; F: time taken by worker ants to find carcasses; G: time taken by worker ants to start carrying carcasses; H: time taken by worker ants to carry all the carcasses. I: Pictures of the digging, foraging, and disposal behavior test. Data are presented as mean \pm SD. Different letters above bars indicate significant differences in behavior-altering among treatments due to nanomaterials effects at $p < 0.05$ level based on Tukey's honestly significant difference (HSD) test ($n = 20$).

IDC content of 0.001 %, the digging weight in the control group was 1.41 g, which was the largest amount of excavation among all treatment groups. and the amounts in the three nanoparticle treatment groups were 0.68, 0.58 and 0.67 g, respectively, with no significant difference. At an IDC content of 0.0025 %, the IDC control had the greatest effect, the digging weight only 0.11 g. There was no significant difference among the three types of CaCO₃-loaded nanoparticles. The inhibitory effect of CaCO₃-loaded nanoparticles on the digging behaviour of worker ants was not greater than that of the IDC TC group, which may be attributed to the reduced exposure of worker ants to IDC as a result of CaCO₃ encapsulation. Pesticide-loaded nanoparticles affected worker ants' carcass abandonment behavior after 24 h of consume. The time taken by OA@IDC@CaCO₃, LA@IDC@CaCO₃, and LNA@IDC@CaCO₃ treatment groups to discover the bodies was 13.00, 11.33 and 9.67 seconds, with no significant difference (Fig. 3F). In terms of time between discovery and moving the carcass, the IDC TC treatment group took the longest time (37.75 s), and there was no significant difference between the three nanoparticles (Fig. 3G). Finally, from the time of discarding the carcasses, the OA@IDC@CaCO₃ treatment group was not significantly different from the IDC TC groups, and the LA@IDC@CaCO₃ and LNA@IDC@CaCO₃ treatment groups presented significantly lower values than the IDC TC group did (Fig. 3H).

3.5. Horizontal transfer of IDC and slow release effect of OA@IDC@CaCO₃

When dead worker carcasses after 24 h of OA@IDC@CaCO₃ and IDC TC treatment were placed with normal feeding worker ants, IDC could be transferred from dead worker carcasses to normal worker ants, causing the death of worker ants. The mortality rate of the IDC TC-treated group was greater than that of the OA@IDC@CaCO₃ group at 1, 2, and 3 d after treatment. (Fig. 4A). This may be attributed to CaCO₃ encapsulation, which slowed the release of IDC, resulting in a decrease in the rate of activity delivery. To confirm this suspicion, the in vitro release behaviour of OA@IDC@CaCO₃ and IDC TC was tested, and the results are shown in Fig. 4B. The cumulative release rate of IDC TC reached 99.98 % after 8 h, whereas the cumulative release rate of OA@IDC@CaCO₃ was only 24.49 %. The cumulative release rate of OA@IDC@CaCO₃ reached 78.45 % after 48 h. The results indicated that the CaCO₃ coating significantly reduced the release rate of IDC.

3.6. Effectiveness of nanomaterials and OA@IDC@CaCO₃ compounding

The highly active nanoadditives DA and MCN previously screened and obtained by our group were compounded with CaCO₃@IDC@OA pesticide-carrying nanoparticles (Ma et al., 2024), and the feeding and

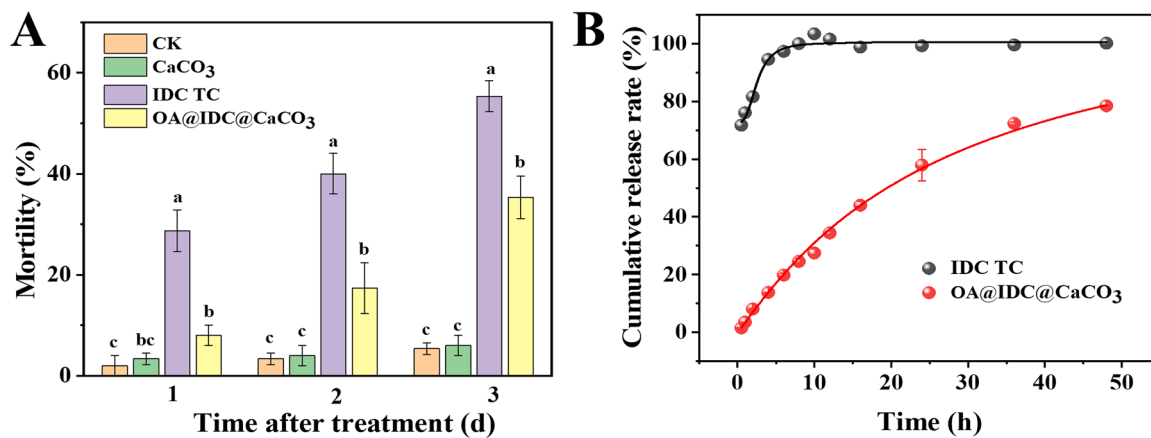


Fig. 4. Efficiency OA@IDC@CaCO₃ of activity transfer among worker ants (A). The cumulative release rate of OA@IDC@CaCO₃ and IDC TC in the acetonitrile-water system at pH= 7 (B). Data are presented as mean \pm SD. Different letters above bars indicate significant differences at the same time among different treatments at $p < 0.05$ level based on Tukey's *t*-test ($n = 20$).

contact activities of the composite formulation were tested, as shown in Fig. 5. According to the results of the contact activity tests, when the concentration of IDC was 0.05 %, after 1 d of contact treatment, almost all the worker ants in the two compound treatment groups died, the mortality rate of the IDC TC group was only 41.33 %, and the mortality rate of the compound group was significantly greater than that of the IDC treatment group (Fig. 5A). At medium concentrations (0.01 % and 0.005 %), the mortality of the two nanomaterials in the first 2 d after exposure to the treatments was greater and significantly different from that of the IDC TC group (Fig. 5B and C); from the 3rd day onwards, The maximum mortality rate of 90.67 % cent was achieved in the DA + OA@IDC@CaCO₃ group, but the difference with the IDC TC group was not significant. At the low concentration (0.0025 %), there was a significant difference between DA + OA@IDC@CaCO₃ group and the other treatments after 3 d treatment, the mortality rate of DA + OA@IDC@CaCO₃ group was 25.33 %. However, there was no significant difference in the MCN compounding group compared with the IDC TC group (Fig. 5D). The results of the contact activity test revealed that DA combined with CaCO₃@IDC@OA had a more obvious synergistic effect than MCN did, especially when the content was low.

The results of the feeding activity tests revealed that when the concentration of the active ingredient was 0.05 %, there was a significant difference in the mortality rates of the different treatment groups after 1 d of feeding (Fig. 5E), with the highest mortality occurring in the MCN + OA@IDC@CaCO₃ group (80.67 %), followed by the DA + OA@IDC@CaCO₃ group (62.00 %) and then the IDC group (38.67 %). However, when the active ingredient concentrations were 0.01 % and 0.005 %, the order of the mortality rate after 1, 2, and 3 d of treatment changed to DA + OA@IDC@CaCO₃, IDC and MCN + OA@IDC@CaCO₃ (Fig. 5F and G). The use of both DA and MCN improved the effectiveness of OA@IDC@CaCO₃ when the active ingredient concentration was 0.0025 % after 4d, the mortality was 48.44 % and 44.00 % in the DA and MCN-added groups, respectively, which was significantly higher than that of 28.67 % in the IDC TC treated group (Fig. 5H). From the above results for DA and MCN with OA@IDC@CaCO₃, the synergistic lethal effect of DA + OA@IDC@CaCO₃ on worker ants was more significant. Therefore, we also assessed the behavioural effects of this combination on worker ants and the lethal effects on larvae.

3.7. Behavioural regulation of DA and OA@IDC@CaCO₃ compounding

The effects of the OA@IDC@CaCO₃ composite and DA bait on the foraging, digging, and carcass disposal behaviour of worker ants are shown in Fig. S3. Compared with the IDC-treated group, the DA + OA@IDC@CaCO₃ treatment groups significantly increased the time it

took for worker ants to find and carry food after 24 h of feeding, while the number of feeding worker ants and food consumption decreased. The DA + OA@IDC@CaCO₃ group took an average of 25.67 s to discover the food, followed by the IDC TC-treated group at 13.33 s and the blank control group at 8.33 s (Fig. S3A). The average time from discovery to the commencement of handling was 249.67 s in the DA+OA@IDC@CaCO₃ group, 154.33 s in the IDC group and 49.33 s in the control group, with significant differences between the treatment groups (Fig. S3B). The number of worker ants that fed and consumed food was also lower in the DA + OA@IDC@CaCO₃ group than in the IDC treatment group (Fig. S3C and D). In terms of digging behaviour, the weight of the sand dug by worker ants was significantly lower in the DA + OA@IDC@CaCO₃ group than in the IDC group at the two active ingredient concentrations of 0.0025 % and 0.001 % (Fig. S3E). Compared with the blank control, both the IDC and the DA + OA@IDC@CaCO₃ treatment groups significantly prolonged the total time required for worker ants to find carcasses, start carrying carcasses, and discard carcasses. The time taken to find carcasses and start handling them was significantly longer in the DA + OA@IDC@CaCO₃ group than in the IDC group (Fig. S3F and G), but the total time taken to handle carcasses was not significantly different between the two treatment groups (Fig. S3H). The carcasses of RIFAs that died after 24 h of exposure to DA + OA@IDC@CaCO₃ were placed with normal worker ants, and the IDC was able to be transferred to the normal worker ants during the exposure process, which resulted in the death of the normal feeding worker ants. The mortality of the DA + OA@IDC@CaCO₃-treated group was significantly greater than that of the IDC TC group after 12, 24, and 36 h of carcass treatment (Fig. S3I). The DA and OA@IDC@CaCO₃ combination increased the mortality rate of normal worker ants after exposure to dead worker ants, improved the efficiency of activity delivery and contributed to more complete population control.

3.8. Lethal activity of DA compounded with OA@IDC@CaCO₃ against larval ants

The contact and feeding activities of DA compounded with OA@IDC@CaCO₃ on larval ants are shown in Fig. S4. After 2 d of contact treatment with 0.15 % active ingredient, the mortality of the DA + OA@IDC@CaCO₃ group was significantly greater than that of the IDC-treated group (Fig. S4A). When the concentration of the active ingredient was 0.01 % or 0.005 %, there was no significant difference between the DA + OA@IDC@CaCO₃ group and the IDC group, and the mortality rate was less than 20 % (Fig. S4 B and C). In terms of feeding activity, the difference in mortality between the DA + OA@IDC@CaCO₃

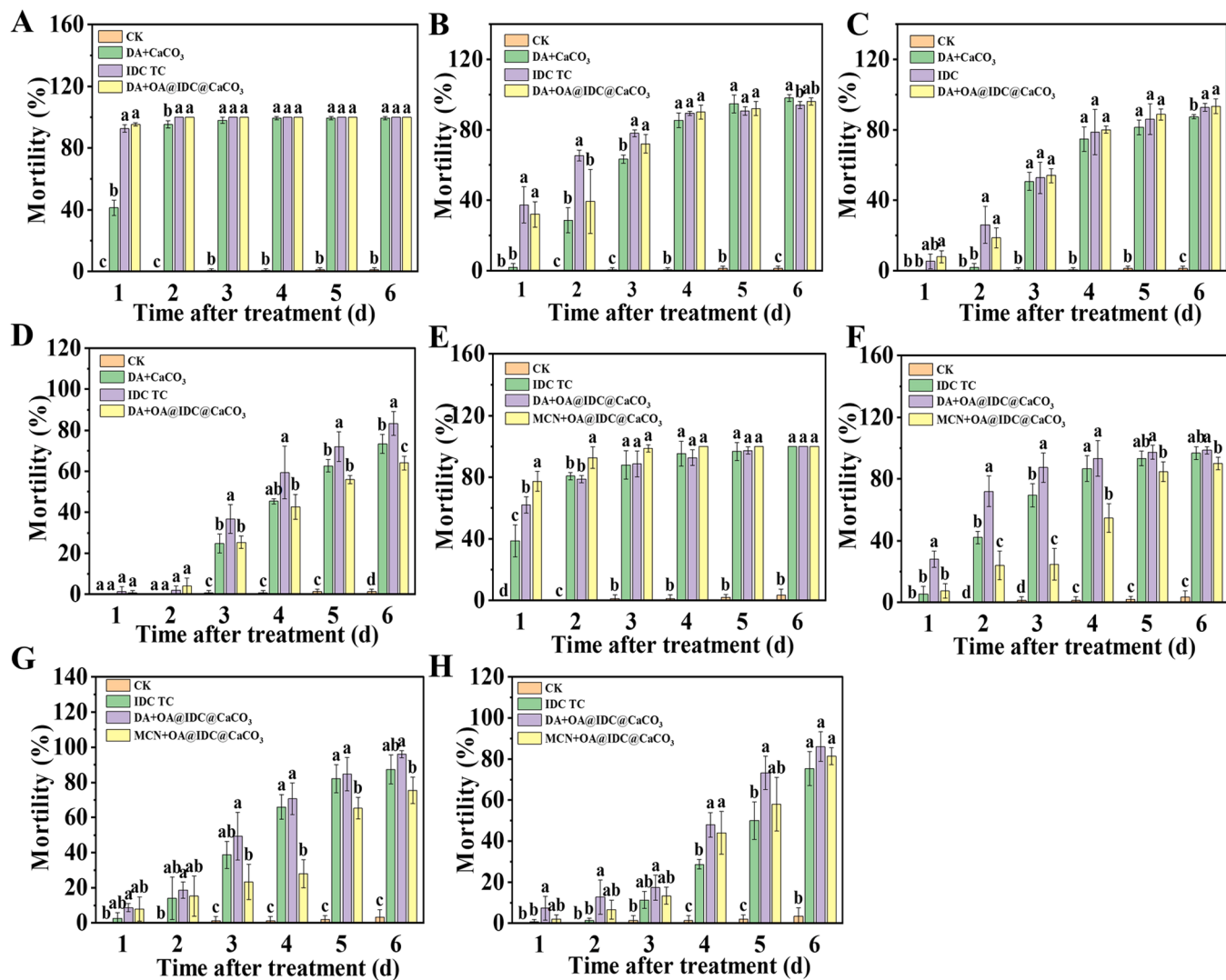


Fig. 5. Mortality of worker ants after 1, 2, 3, 4, 5, and 6 d of contact and feeding exposure at concentrations of 0.05, 0.01, 0.005, and 0.0025 % IDC in the compounded baits. A: Mortality after contact treatments with different bait concentrations of IDC at 0.05 %. B: Mortality after contact treatments with different bait concentrations of IDC at 0.01 %. C: Mortality after contact treatments with different bait concentrations of IDC at 0.005 %. D: Mortality after contact treatments with different bait concentrations of IDC at 0.0025 %. E: Mortality of worker ants of feeding exposure to active ingredient (IDC) at a concentration of 0.05 %. F: Mortality of worker ants of feeding exposure to active ingredient (IDC) at a concentration of 0.01 %. G: Mortality of worker ants of feeding exposure to the active ingredient (IDC) at a concentration of 0.005 %. H: Mortality of worker ants of feeding exposure to the active ingredient (IDC) at a concentration of 0.0025 %. Data are presented as mean \pm SD. Different letters above bars indicate significant differences in mortality rate at the same time among treatments due to nanomaterials effects at $p < 0.05$ level based on Tukey's *t*-test ($n = 20$).

group and the IDC group was not significant at the 0.05 % active ingredient concentration (Fig. S4D). When the concentrations of the active ingredients were 0.01 % and 0.005 %, the mortality rate of the larval ants significantly increased on the 3rd and 4th days after feeding, respectively (Fig. S4E and F). The results indicated that the combination of DA and OA@IDC@CaCO₃ improved the feeding activity of larval ants under low-concentration conditions.

3.9. Field control effects of DA and OA@IDC@CaCO₃

We evaluated the effectiveness of the DA and OA@IDC@CaCO₃ compound baits on nests and worker ants in the field, excavated the nests after the last baiting, counted the colony levels and calculated the combined control effect; some of the experimental field pictures are presented in Fig. 6A. After 7 d and 14 d of application, the commercial agent (IDC) and the compound baits had excellent control effects on the live ant nests, with control efficacies above 92.86 %. However, after 21 and 28 d of application, the control effects of IDC were 46.11 % and

35.76 %, respectively, and the control effects of the compound baits were 76.91 % and 71.45 %, which were significantly greater than those of the commercial agent control group (Fig. 6B). After 7, 14, 21 and 28 d of application, the efficacy of both the commercial baits and the compound baits in the compounded treatment groups against worker ants exceeded 90 %, and there was no significant difference between the two groups for the same treatment time (Fig. 6C). On the 28th day after the treatment, the treated nests were excavated, and the surviving RIFAs were observed. Only a small number of worker ants survived in the nests of the commercial control group and compounded bait group, no other forms of RIFAs, such as juvenile ants and reproductive ants, were found, and the efficacies against the ant colony were 85.19 % and 92.59 %, respectively, with no significant difference between the two groups. The comprehensive control of RIFAs in the compounded bait treatment group reached 83.38 %, which was higher than the 69.65 % in the commercial agent control group (Fig. 6D). The results of the field experiment indicated that the DA+ OA@IDC@CaCO₃ compound bait in this study had a longer persistence period, and the control effect on

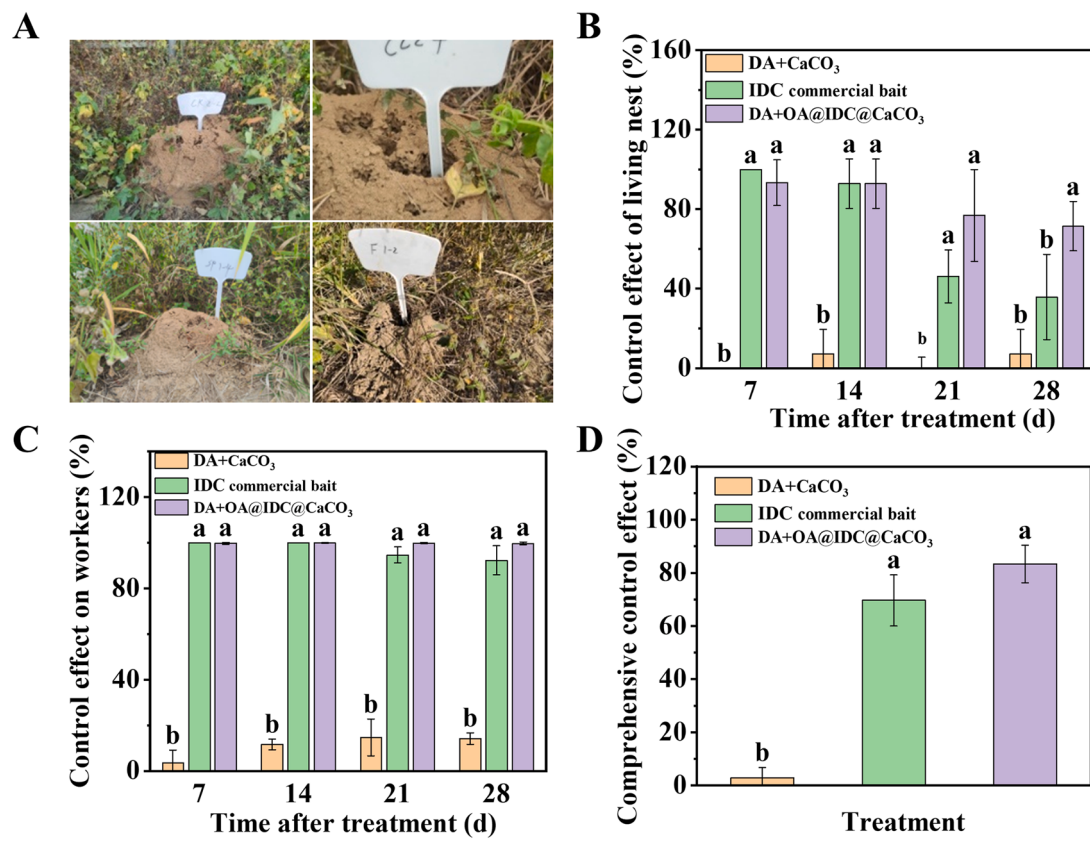


Fig. 6. Efficacy of DA and OA@IDC@CaCO₃ compounded baits for field control of RIFAs. A: Pictures of the field trial site. B: Control effects of ant nests. C: Control effects of worker ants. D: Comprehensive control effect. Data are presented as mean \pm SD. Different letters above bars indicate significant differences at the same time among different treatments at $p < 0.05$ level based on Tukey's *t*-test ($n = 3$).

RIFAs was greater than that of the commercial agent.

4. Discussion

Infestations of RIFAs are severe and difficult to eradicate. Chemical pesticides are still the primary means of preventing and controlling RIFAs, with IDC being one of the most commonly used pesticides. The extensive use of chemicals is harmful to the environment, nontarget organisms, and human health. In addition, IDC is insoluble in water, and nanoloading against IDC often requires the use of large amounts of organic solvents, which is not ecologically friendly. In this study, we prepared IDC DESs using OA, LA and LNA, and designed a CaCO₃ coated nano IDC-carrying systems, we aimed to achieve efficient control of RIFAs and reduce the application of chemical pesticides.

The use of conventional organic solvents (methanol, ethanol, etc.) has several disadvantages, including high dosage, high toxicity, high volatility, and environmental unfriendliness. As ecological and environmental protection become more widely recognized and solvent control becomes more stringent, DESs have gained a lot of attention across a range of industries. DESs have superior solubility and thermal stability than conventional organic solvents, and they are typically manufactured from low-cost, low-toxicity basic ingredients. As consequence, they are widely sought after and used in a variety of industries. Solubility screening of DESs was conducted to select suitable candidates. Multiple studies have demonstrated a relationship between the solubility and the compositions and properties of DESs (Azzouz and Hayyan, 2023). Our findings show that the use of OA LA and LNA as dissolved solvents leads to superior results, potentially due to their high electronegativity, which facilitates hydrogen bond formation with IDC. This, in turn, enhances the solubility in a range of DES compositions. However, in our study, the difference in solubility among OA, LA, and LNA was not

significant. Therefore, IDC, OA, LA, and LNA were prepared as DES. In recent years, DES have been widely used in nanotechnology as media, reactants, templates, functionalizers, and dispersants. The use of DESs as templates for the synthesis of nanoparticles has been reported. Karimi et al. developed a sustainable and cost-effective method for the synthesis of copper-zinc-tin chalcogenide nanoparticles by using a DES consisting of choline chloride: urea (molar ratio = 1:2) as a solvent and template (Karimi et al., 2016). Mn₃O₄ nanoparticles can be synthesized by a simple and sustainable method using DES (glycol-choline chloride), which plays a triple role of solvent, reactant, and template in the synthesis process (Karimi and Eshraghi, 2017). Albayati et al. prepared nanoparticles with a metal-organic backbone (UiO-66) via a solvothermal method using a green DES solvent consisting of choline chloride and urea, and the nanoparticles formed by DESs were smaller in size and had a lower surface area than those prepared via the conventional solvent dimethylformamide (Albayati and Kadhom, 2020). Chen et al. reported that poly(ethylene glycol) and hydroxide can form a new series of green, low-cost DESs, which can be used to prepare cubic NiCo₂O₄ ultrathin nanosheets at 80 °C with extreme simplicity, speed, and energy efficiency (Chen et al., 2020). DES was prepared by Samage et al. using three solvents, namely, a reducing agent, a template, and a source for the preparation of cobalt-manganese oxides at room temperature (Samage et al., 2023).

Furthermore, the advancement of nanotechnology has significantly transformed the field of agricultural sciences, particularly in the development of nano-delivery systems for pesticides. These systems capitalize on the unique physicochemical properties of nanomaterials, leading to enhanced efficacy and reduced environmental impact compared to conventional pesticides. We designed a DES-CaCO₃ system to increase the lethal activity and behavioral regulation effects on RIFAs. The DES-CaCO₃ system was synthesized using DESs as templates to reduce

the number of organic solvents. Three kinds of nanoparticles, OA@IDC@CaCO₃, LA@IDC@CaCO₃, and LNA@IDC@CaCO₃, were prepared using CaCO₃ for coating without the need for a complex postloading process, simplifying the encapsulation process. IDC, CaCO₃, OA@IDC@CaCO₃, LA@IDC@CaCO₃, and LNA@IDC@CaCO₃ were fed to workers to investigate the effects of nanoparticles on the insecticidal activity and feeding behaviour of worker ants. RIFAs are social insects with a wide variety of colony behaviours that sustain the colony (Starkey and Tamborindeguy, 2023). Feeding, digging, and carcass disposal are behaviours that are necessary to maintain a functioning population. Foraging is necessary to maintain basic survival (Roeder et al., 2020). The main purpose of digging is to build nests that provide space for RIFAs to survive, reproduce, and store food (Chen, 2021), and carcass abandonment protects live ants from infections such as pathogens associated with carcasses (Zhang et al., 2022). In this study, the feeding activity of the three pesticide-loaded nanoparticles against worker ants was assessed via an indoor activity assay, which revealed that the activity increased at low concentrations compared with that of IDC TC and significantly inhibited the behaviour of worker ants, with OA@CaCO₃@IDC being relatively more effective. The in vitro release test also revealed that the use of CaCO₃ for coating has a slow-release effect, which can slow the degradation process of IDC and prolong its holding period.

For RIFAs control, chemical baiting is widely used because of its ease of use and excellent control effect. Chemical baits are usually composed of three parts: an insecticide, a vegetable oil lure (soybean oil, etc.), and an insecticide carrier (usually cornstarch), and the preparation process is relatively simple (Wang et al., 2020). In recent years, with the development of nanotechnology, nanocarriers, as novel technologies, have also been introduced into RIFAs baits. He et al. used alloy nanomaterials to improve the control of RIFAs (He et al., 2023a). Zheng et al. prepared chitosan-fisetidone nanobaits with acid-responsive release properties (Zheng et al., 2022). Yang et al. enhanced the insecticidal activity of IDC by synthesizing a β-cyclodextrin-functionalized metal organ skeleton functionalized with β-cyclodextrin to affect the amino acid metabolism of RIFAs to increase the insecticidal activity of IDC (Yang et al., 2023).

Many nanomaterials have been shown to have insecticidal activity. Nanomaterials are used in pest control in the following ways: first, nanomaterials are used as active insecticidal ingredients directly for pest control (Cáceres et al., 2019); second, nanomaterials are used as bio-stimulants to confer resistance to plant pathogens or pests; and third, nanomaterials are used as carriers of active pesticide ingredients to construct nano pesticide-carrying systems (Kumar et al., 2019). DA, which is mainly composed of SiO₂, is a kind of fossil formed by the deposition of algal plants and is a natural insecticide and a common additive in pesticide production (Nilpay, 2006). Its insecticidal mechanism is mainly to cause insects to lose water and die because of the friction of their particles with their epidermis, which damages the wax layer of the epidermis (Mewis and Ulrichs, 2001). DA is stable and does not produce toxic chemical residues or react with substances in the environment. In this study, DA and OA@CaCO₃@IDC were further compounded and applied to baits to improve feeding and contact activity, significantly inhibiting the foraging, digging, and carcass disposal behaviours of worker ants compared with IDC TC. Field trials also demonstrated that the combination of DA and OA achieved better efficacy than commercial agents. After 28 d, the comprehensive control effect of DA + OA@CaCO₃@IDC treatment group was 83.38 %, which was higher than that of IDC commercial agent of 69.65 %. After digging up the RIFAs nests, a small number of worker ants were discovered in the treatment group of the IDC commercial bait, which was most likely due to the commercial agent's failure to completely eliminate the larvae and pupa, resulting in the re-incubation of worker ants in the nests at a later stage of time and incomplete control. The field test reconfirmed that the combination of DA and the IDC-carrying system developed in this work enhanced the control effect and extended the period of efficacy against

RIFAs.

In summary, the results of this study showed that the prepared DESs were coated with CaCO₃, which could slow the degradation process of IDC and prolong its efficacy. OA@IDC@CaCO₃ was compounded with DA, which significantly improved the contact and feeding activity of worker and larval ants, as well as the activity transfer between populations. Further studies on the mechanism of the synergistic effect of DESs and DA will be carried out subsequently.

5. Conclusion

In this study, IDC, OA, LA, and LNA were mixed to prepare DESs, and three types of monolayer microcapsules were prepared and formed using DESs as a template and encapsulated in CaCO₃ (OA@IDC@CaCO₃, LA@IDC@CaCO₃ and LNA@IDC@CaCO₃). The feeding activity of these three pesticide-loaded nanoparticles on worker ants was evaluated via an indoor activity assay. Compared with IDC, OA@IDC@CaCO₃, LA@IDC@CaCO₃, and LNA@IDC@CaCO₃ increased the lethal activity, significantly inhibited carcass disposal and foraging behaviours, and reduced the number of feeding workers and the food consumption of worker ants. The OA@IDC@CaCO₃-loaded nanoparticles were compounded with DA to improve the activity against worker and larval ants. Compared with the IDC formulation, the addition of DA resulted in an increase in the activity delivery efficiency of the complex formulation and significantly inhibited the colony behaviour of RIFAs. A field trial also revealed that the combination of OA@IDC@CaCO₃ and DA was more effective than the commercial agent. This study provides technical support for RIFAs prevention and control.

Ethical approval and consent to participate

No approval of research ethics committees was required to accomplish the goals of this study because the experimental work was conducted with an unregulated invertebrate species.

Funding

This study was supported by the Hainan Province Science and Technology Species Fund (ZDYF2022XDNY138), Guangdong Province Key R&D Programme Projects (2023B0202080001), Hainan Provincial Natural Science Foundation of China (324RC454), Young Talent Project of GDAS (2023GDASQNRC-0307), and China Agriculture Research System of Sugar (CARS-170306). The authors would like to thank all organizations that funded our research.

CRediT authorship contribution statement

Yanping Luo: Writing – review & editing, Funding acquisition. **Jiantao Fu:** Writing – original draft, Formal analysis, Data curation. **Yunfei Zhang:** Formal analysis, Data curation. **Lanying Wang:** Validation, Software. **Junfang Wang:** Investigation, Formal analysis. **Zewen Ma:** Software, Methodology, Data curation.

Declaration of Competing Interest

The authors declare that they have no conflicts of interest regarding the submission of this manuscript, and the manuscript is approved by all authors for publication.

Appendix A. Supporting information

Supplementary data associated with this article can be found in the online version at doi:10.1016/j.ecoenv.2025.117709.

Data availability

Data will be made available on request.

References

- Abro, R., Kiran, N., Ahmed, S., Muhammad, A., Jatoi, A.S., Mazari, S.A., Plechkova, N.V., 2022. Extractive desulfurization of fuel oils using deep eutectic solvents—a comprehensive review. *J. Environ. Chem. Eng.* 10 (3), 107369.
- Albayati, N., Kadhom, M., 2020. Preparation of functionalised UiO-66 metal–organic frameworks (MOFs) nanoparticles using deep eutectic solvents as a benign medium. *Mater. Nano Lett.* 15 (15), 1075–1078.
- Alves, K.V.B., Martinez, D.S.T., Alves, O.L., Barbieri, E., 2022. Co-exposure of carbon nanotubes with carbofuran pesticide affects metabolic rate in *Palaemon pandaliformis* (shrimp). *Chemosphere* 288, 132359.
- Azzouz, A., Hayyan, M., 2023. Potential applications of deep eutectic solvents in nanotechnology: part II. *Chem. Eng. J.* 468, 143563.
- Basar, A.O., Prieto, C., Durand, E., Villeneuve, P., Sasimazel, H.T., Lagaron, J., 2020. Encapsulation of β-carotene by emulsion electrospraying using deep eutectic solvents. *Molecules* 25 (4), 981.
- Bertelsmeier, C., Ollier, S., Liebhold, A., Keller, L., 2017. Recent human history governs global ant invasion dynamics. *Nat. Ecol. Evol.* 1 (7), 0184.
- Bilal, M., Xu, C., Cao, L., Zhao, P., Cao, C., Li, F., Huang, Q., 2020. Indoxacarb-loaded fluorescent mesoporous silica nanoparticles for effective control of *Plutella xylostella* L. with decreased detoxification enzymes activities. *Pest Manag. Sci.* 76 (11), 3749–3758.
- Cáceres, M., Vassena, C.V., Garcerá, M.D., Santo-Orihuela, P.L., 2019. Silica nanoparticles for insect pest control. *Curr. Pharm. Des.* 25 (37), 4030–4038.
- Cao, J., Su, E., 2021. Hydrophobic deep eutectic solvents: the new generation of green solvents for diversified and colorful applications in green chemistry. *J. Clean. Prod.* 314, 127965.
- Chen, J., 2021. Evidence of social facilitation and inhibition in digging behavior of red imported fire ants, *Solenopsis invicta*. *Insect Sci.* 28, 566–570.
- Chen, J., Ali, M.C., Liu, R., Munyemana, J.C., Li, Z., Zhai, H., Qiu, H., 2020. Basic deep eutectic solvents as reactant, template and solvents for ultra-fast preparation of transition metal oxide nanomaterials. *Chin. Chem. Lett.* 31 (6), 1584–1587.
- Chen, H., Zhao, Y., Zhao, T., Li, Y., Ren, B., Liang, H., Liang, H., 2023. Multi-walled carbon nanotubes enhance the toxicity effects of dibutyl phthalate on early life stages of zebrafish (*Danio rerio*): research in physiological, biochemical and molecular aspects. *Sci. Total Environ.* 899, 165684.
- Collignon, R.M., Siderhurst, M.S., Cha, D.H., 2023. Evidence of queen-rearing suppression by mature queens in the little fire ant, *Wasmannia auropunctata*. *Insectes Soc.* 70 (2), 259–263.
- Dantas, J.O., Cavalcanti, S.C., Araújo, A.P.A., Blank, A.F., Silva, J.E., Picanço, M.C., Bacci, L., 2023. Synthetic carvacrol derivatives for the management of *Solenopsis* Ants: toxicity, sublethal effects, and horizontal transfer. *Agriculture* 13 (10), 1988.
- El Achkar, T., Greige-Gerges, H., Fourmentin, S., 2021. Basics and properties of deep eutectic solvents: a review. *Environ. Chem. Lett.* 19, 3397–3408.
- Fukamachi, K., Konishi, Y., Nomura, T., 2019. Disease control of phytophthora infestans using cyazofamid encapsulated in poly lactic-co-glycolic acid (PLGA) nanoparticles. *Colloids Surf. A* 577, 315–322. <https://doi.org/10.1016/j.colsurfa.2019.05.077>.
- Gruber, M.A., Santoro, D., Cooling, M., Lester, P.J., Hoffmann, B.D., Boser, C., Lach, L., 2022. A global review of socioeconomic and environmental impacts of ants reveals new insights for risk assessment. *Ecol. Appl.* 32 (4), e2577.
- He, M., Zhang, T., Chen, Q., Gong, C., Pu, J., Yang, J., Wang, X., 2023a. NiCoNC nanoenzyme enhances the performance of insecticides against *Solenopsis invicta* by inhibiting the gene expression of P450. *Chem. Eng. J.* 474, 145569.
- He, Y., Zhang, J., Shen, L., Wang, L., Qian, C., Lyu, H., Wang, C., 2023b. Eugenol derivatives: strong and long-lasting repellents against both undisturbed and disturbed red imported fire ants. *J. Pest Sci.* 96 (1), 327–344.
- Huang, Y., Chen, S., Li, Z., Wang, L., Xu, Y., 2018. Effects of flavor enhancers on the survival and behavior of the red imported fire ant, *Solenopsis invicta* (Hymenoptera: Formicidae). *Environ. Sci. Pollut. Res.* 25, 21879–21886.
- Jaleel, W., Li, Q., Khan, K.A., Khan, F.R., Ullah, F., Azad, R., Lihua, L.Y.U., 2021. Optimization of treatment blocking the gustatory sense and feeding ethogram of red imported fire ant, *Solenopsis invicta* Buren (Hymenoptera: Formicidae) to sugar. *J. King Saud Univ. Sci.* 33 (7), 101555.
- Karimi, M., Eshraghi, M.J., 2017. One-pot and green synthesis of Mn₃O₄ nanoparticles using an all-in-one system (solvent, reactant and template) based on ethaline deep eutectic solvent. *J. Alloys Compd.* 696, 171–176.
- Karimi, M., Eshraghi, M.J., Jahangir, V., 2016. A facile and green synthetic approach based on deep eutectic solvents toward synthesis of CZTS nanoparticles. *Mater. Lett.* 171, 100–103.
- Kumar, S., Nehra, M., Dilbaghi, N., Marrazza, G., Hassan, A.A., Kim, K.H., 2019. Nano-based smart pesticide formulations: emerging opportunities for agriculture. *J. Control. Release* 294, 131–153.
- Lei, W.A.N.G., XU, Y.J., Ling, Z.E.N.G., LU, Y.Y., 2019. Impact of the red imported fire ant *Solenopsis invicta* Buren on biodiversity in South China: a review. *J. Integr. Agric.* 18 (4), 788–796.
- Li, M., Cui, H., Cao, Y., Lin, Y., Yang, Y., Gao, M., Wang, C., 2023b. Deep eutectic solvents—hydrogels for the topical management of rheumatoid arthritis. *J. Control. Release* 354, 664–679.
- Li, C., Sheng, X., Li, N., Ping, Q., Lu, P., Zhang, J., 2022. Insecticidal characteristics and mechanism of a promising natural insecticide against saw-toothed grain beetle. *RSC Adv.* 12 (12), 7066–7074.
- Li, L., Wu, X., Pang, Y., Lou, H., Li, Z., 2023a. In situ encapsulation of cytochrome c within covalent organic frames using deep eutectic solvents under ambient conditions. *ACS Appl. Mater. Interfaces* 15 (46), 53871–53880.
- Ma, Z., Fu, J., Zhang, Y., Wang, L., Luo, Y., 2024. Toxicity and behavior-altering effects of three nanomaterials on red imported fire ants and their effectiveness in combination with indoxacarb. *Insects* 15, 96.
- Menchetti, M., Schifani, E., Alicata, A., Cardador, L., Sbrega, E., Toro-Delgado, E., Vila, R., 2023. The invasive ant *Solenopsis invicta* is established in Europe. *Curr. Biol.* 33 (17), R896–R897.
- Mewis, I., Ulrichs, C., 2001. Action of amorphous diatomaceous earth against different stages of the stored product pests *Tribolium confusum*, *Tenebrio molitor*, *Sitophilus granarius* and *Plodia interpunctella*. *J. Stored Prod. Res.* 37 (2), 153–164.
- Mou, H., Wang, J., Yu, D., Zhang, D., Lu, F., Chen, L., Mu, T., 2019. A facile and controllable, deep eutectic solvent aided strategy for the synthesis of graphene encapsulated metal phosphides for enhanced electrocatalytic overall water splitting. *J. Mater. Chem. A* 7 (22), 13455–13459.
- Nikpay, A., 2006. Diatomaceous earths as alternatives to chemical insecticides in stored grain. *Insect Sci.* 13 (6), 421–429.
- Ning, D., Hassan, B., Nie, L., Yang, K., Pan, Y., Pan, Z., Xu, Y., 2020. L-ascorbic acid provides a highly effective and environmentally sustainable method to control red imported fire ants. *J. Pest Sci.* 93, 879–891.
- Ning, D., Yang, F., Xiao, Q., Ran, H., Xu, Y., 2019. A simple and efficient method for preventing ant escape (Hymenoptera: Formicidae). *Myrmecol. N.* 29, 57–65.
- Omar, K.A., Sadeghi, R., 2023. Database of deep eutectic solvents and their physical properties: a review. *J. Mol. Liq.* 121899.
- Roeder, K.A., Prather, R.M., Paraskevopoulos, A.W., Roeder, D.V., 2020. The economics of optimal foraging by the red imported fire ant. *Environ. Entomol.* 49 (2), 304–311.
- Samage, A., Pramoda, K., Halakarni, M., Sanna Kotrappanavar, N., 2023. One-step rapid conversion of electroactive CoMnO nanostructures using a deep eutectic solvent as the template, solvent, and source. *ACS Appl. Energy Mater.* 6 (4), 2412–2422.
- Shah, B., Sonkusale, S., Owyang, R., 2024. Development of deep eutectic solvent systems and their formulation: assessment of solubilization potential on poorly water-soluble drugs. *MRS Commun.* 1–9.
- Silva, J.M., Silva, E., Reis, R.L., 2021. Therapeutic deep eutectic solvents assisted the encapsulation of curcumin in alginate-chitosan hydrogel beads. *Sustain. Chem. Pharm.* 24, 10053.
- Standardization Administration of the People's Republic of China. GBT 17980.149-2009 Pesticide Field Efficacy Test Guideline (II) Part 149: Insecticide Control of Red Fire Ants.
- Starkey, J., Tamborindeguy, C., 2023. Family before work: task reversion in workers of the red imported fire ant, *Solenopsis invicta* in the presence of brood. *Sci. Rep.* 13, 2379.
- Wang, L., Zeng, L., Xu, Y., Lu, Y., Xuv, Y., 2020a. Prevalence and management of *Solenopsis invicta* in China. *NeoBiota* 54, 89–124.
- Wang, L., Zeng, L., Xu, Y., Lu, Y., 2020. Prevalence and management of *Solenopsis invicta* in China. *NeoBiota* 54, 89–124.
- Wing, K.D., Sacher, M., Kagaya, Y., Tsurubuchi, Y., Mulderig, L., Connair, M., Schnee, M., 2000. Bioactivation and mode of action of the oxadiazine indoxacarb in insects. *Crop Prot.* 19 (8–10), 537–545.
- Xu, Y., Vargo, E.L., Tsuji, K., Wylie, R., 2022. Exotic ants of the Asia-Pacific: invasion, national response, and ongoing needs. *Annu. Rev. Entomol.* 67 (1), 27–42.
- Yang, L., Chen, H., Zheng, Q., Luo, P., Yan, W., Huang, S., Zhang, Z., 2023. A β-cyclodextrin-functionalized metal–organic framework enhances the insecticidal activity of indoxacarb by affecting amino acid metabolism in red imported fire ants. *Chem. Eng. J.* 458, 141417.
- Zhang, L., Wang, L., Chen, J., Zhang, J., He, Y., Lu, Y., Wang, C., 2022. Toxicity, horizontal transfer, and physiological and behavioral effects of cycloxyaprid against *Solenopsis invicta* (Hymenoptera: Formicidae). *Pest Manag. Sci.* 78 (6), 2228–2239.
- Zheng, Q., Qin, D., Wang, R., Yan, W., Zhao, W., Shen, S., Zhang, Z., 2022. Novel application of biodegradable chitosan in agriculture: using green nanopesticides to control *Solenopsis invicta*. *Int. J. Biol. Macromol.* 220, 193–203.
- Zheng, Q., Wang, R., Qin, D., Yang, L., Lin, S., Cheng, D., Zhang, Z., 2021. Insecticidal efficacy and mechanism of nanoparticles synthesized from chitosan and carboxymethyl chitosan against *Solenopsis invicta* (Hymenoptera: Formicidae). *Carbohydr. Polym.* 260, 117839.